Eur Biophys J (2005) 34: 52–66
DOI 10.1007/s00249-004-0424-1

ARTICLE

Cornelia Schroeder · Harald Heider
Elisabeth Möncke-Buchner · Tse-I Lin

The influenza virus ion channel and maturation cofactor M2 is a cholesterol-binding protein

Received: 15 September 2003 / Revised: 6 March 2004 / Accepted: 19 May 2004 / Published online: 25 June 2004

Abstract The influenza-virus M2 protein has proton channel activity required for virus uncoating and maturation of hemagglutinin (HA) through low-pH compartments. The proton channel is cytotoxic in heterologous expression systems and can be blocked with rimantadine. In an independent, rimantadine-resistant function, M2, interacting with the M1 protein, controls the shape of virus particles. These bud from cholesterol-rich membrane rafts where viral glycoproteins and matrix (M1)/RNP complexes assemble. We demonstrate that M2 preparations from influenza virus-infected cells and from a baculovirus expression system contain 0.5–0.9 molecules of cholesterol per monomer. Sequence analyses of the membrane-proximal M2 endodomain reveal interfacial hydrophobicity, a cholesterol-binding motif first identified in peripheral benzodiazepine receptor and human immunodeficiency virus gp41, and an overlapping phosphatidylinositol 4,5-bisphosphate-binding motif. M2 induced rimantadine-reversible cytotoxicity in intrinsically cholesterol-free *E. coli*, and purified *E. coli*-expressed M2 functionally reconstituted into cholesterol-free liposomes supported rimantadine-sensitive proton translocation. Therefore, cholesterol was nonessential for M2 ion-channel function and cytotoxicity and for the effect of rimantadine. Only about 5–8% of both M2 preparations, regardless of cholesterol content, associated with detergent-resistant membranes. Cholesterol affinity and palmitoylation, in combination with a short transmembrane segment suggest M2 is a peripheral raft protein. Preference for the raft/non-raft interface may determine colocalization with HA during apical transport, the low level of M2 incorporated into the viral envelope and its undisclosed role in virus budding for which a model is presented. M2 may promote clustering and merger of rafts and the pinching-off (fission) of virus particles.

Keywords M2 ion-channel protein · Peripheral raft protein · Virus budding · Membrane fission · Influenza virus

Abbreviations CRAC: Cholesterol recognition/interaction amino acid consensus · DMPC: L-α-dimyristoylphosphatidylcholine · DRM: Detergent-resistant membrane · HA: Hemagglutinin · HDL: High-density lipoprotein · KPS: Potassium phosphate buffer with K_2SO_4 · LDL: Low-density lipoprotein · MDCK: Madin-Darby canine kidney · NA: Neuraminidase · NaPS: Sodium phosphate buffer with Na_2SO_4 · Ni-NTA: Nickel-nitrilotriacetic acid · OG: *N*-octyl-β-D-glucopyranoside · PM: Plasma membrane · PS: Phosphatidylserine · RNP: Ribonucleoprotein · *Sf9*: *Spodoptera frugiperda* · TDC: Taurodeoxycholate · TGN: *trans*-Golgi network · TM: Transmembrane · *T. ni*: *Trichoplusia ni* · TX-100: Triton X-100 · Φ: Hydrophobic amino acid

C. Schroeder
Abteilung Virologie, Institut für Mikrobiologie und Hygiene, Universität des Saarlandes, Homburg/Saar, 66421 Homburg, Germany

Present address: C. Schroeder (✉)
Jadolabs GmbH, Pfotenhauerstr. 108, 01307 Dresden, Germany
E-mail: cornelia.schroeder@jadolabs.com
Fax: +49-351-7963810

H. Heider · E. Möncke-Buchner · T.-I. Lin
Institut für Virologie, Universitätsklinikum Charité, Humboldt-Universität zu Berlin, 10098 Berlin, Germany

Present address: T.-I. Lin
Tibotec BVDV, 2800 Mechelen, Belgium

Introduction

The influenza A virus M2 protein is a minor protein of the viral envelope (Zebedee and Lamb 1988) forming an ion channel (Pinto et al. 1992) which is proton-selective (Schroeder et al. 1994a; Chizhmakov et al. 1996; Mould et al. 2000; Lin et al. 2001). M2 is a tetrameric type III integral membrane protein with a 24-amino acid ecto-

domain, a 19-amino acid transmembrane domain, and a 53-amino acid endodomain with palmitate and phosphate modifications (Sugrue et al. 1990a; Holsinger and Lamb 1991; Parks and Lamb 1991; Sugrue and Hay 1991; Veit et al. 1991; Holsinger et al. 1995). The ion-channel function, which is essential for the infectious cycle (Takeda et al. 2002), mediates viral entry and the transit of acid-labile viral hemagglutinins through low-pH compartments (cf. reviews Hay 1992 and Lamb et al. 1994). During viral entry, M2 is envisaged to conduct protons from the acidified endosome lumen into the virion to dissociate the virus matrix (uncoating), a prerequisite to nuclear transport of the ribonucleoprotein (RNP) and subsequent viral gene expression (for reviews see Whittaker et al. 1996; Whittaker and Helenius 1998). To escape premature low pH-induced conformational transition of postsynthetically activated, metastable hemagglutinin (HA), certain H5 and H7 influenza viruses critically depend on M2-mediated proton efflux from the *trans*-Golgi (Sugrue et al. 1990b; Ciampor et al. 1992a, 1992b; Grambas et al. 1992; Ohuchi et al. 1994; Takeuchi and Lamb 1994). M2 is not only the prototype viral ion-channel protein (for a recent review, see Fischer and Sansom 2002) but a multifunctional protein involved in virus assembly (Hughey et al. 1995). Interactions between the M2 and the M1 (matrix) protein control the morphology of virus budding (filamentous vs. spherical; Hughey et al. 1995; Roberts et al. 1998). Inasmuch as this process is not affected by the antiviral ion-channel blocker amantadine (Zebedee and Lamb 1989), the M2 ion channel seems not to be involved.

Detergent-resistant cholesterol- and sphingolipid-rich membrane microdomains (DRM or rafts) are implicated in the budding of ortho- and paramyxo-, retro- and other viruses (Sanderson et al. 1995; Scheiffele et al. 1999; Manié et al. 2000; Zhang et al. 2000b; for reviews see Pickl et al. 2001; Nayak and Barman 2002; Briggs et al. 2003). In polarized host cells, the three influenza A-virus envelope proteins HA, neuraminidase (NA) and M2 express apically and co-localize in the *trans*-Golgi (Zebedee et al. 1985; Hughey et al. 1992; Kundu et al. 1996). HA and NA sequester to rafts (Skibbens et al. 1989; Kurzchalia et al. 1992; Kundu et al. 1996; Scheiffele et al. 1997; Harder et al. 1998) which associate with viral matrix–RNP complexes (Zhang et al. 2000b; Barman et al. 2001). The raft content of influenza-virus envelope is close to 100% (Scheiffele et al. 1999; Zhang et al. 2000b). Despite equal abundance of HA and M2 on the PM (Zebedee et al. 1985), only a small proportion of the M2 protein partitions into DRM (Zhang et al. 2000b), correlating with its near exclusion from the virus envelope, which contains approximately 500 HA spikes but only 16–67 M2 monomers (Zebedee and Lamb 1988).

Proteins are targeted to rafts by specific membrane-spanning sequences and by covalent lipid modifications such as a GPI anchor or saturated fatty acids (reviews: Simons and Ikonen 1997; Brown and London 1998; Harder et al. 1998; Scheiffele et al. 1999; Melkonian et al. 1999). Cholesterol, a key raft constituent essential for trafficking HA from the *trans*-Golgi network (TGN) to the apical surface (Keller and Simons 1998), can itself serve as a protein-associated raft-targeting signal. For example, caveolin binds about one cholesterol molecule per polypeptide chain tightly though noncovalently (Murata et al. 1995). During self-splicing, sonic hedgehog (Shh) protein attaches cholesterol covalently to its signaling domain (Porter et al. 1996), enabling the protein to move into membrane rafts (Rietveld et al. 1999) and between cells as a morphogen (reviewed in Ingham 2000). Several viral and host membrane proteins bind cholesterol specifically but less strongly than Shh and caveolin, e.g. Sendai virus F protein (Asano and Asano 1988), HIV gp41 (Vincent et al. 2002), the peripheral benzodiazepine receptor (Li and Papadopoulos 1998), and synaptophysin (Thiele et al. 2000) to mention a few. Both caveolin and Shh are also palmitoylated (Monier et al. 1996; Pepinsky et al. 1998), as are influenza M2 (Sugrue et al. 1990a; Veit et al. 1991) and hemagglutinin (Schmidt 1982). Hemagglutinin is targeted to rafts by its C-terminal membrane anchor (Scheiffele et al. 1997; Lin et al. 1998; Armstrong et al. 2000) but efficient raft association appears to require palmitoylation at all three positions within the TM anchor and the adjacent cytoplasmic tail (Melkonian et al. 1999).

The M2 protein dissipates pH gradients at the PM and TGN (Ciampor et al. 1992a, 1992b; Grambas and Hay 1992). On heterologous expression in vertebrate cells, M2 slows down protein traffic (including its own) through the Golgi complex and delays apical transport from the TGN (Sakaguchi et al. 1996; Henkel and Weisz 1998; Henkel et al. 2000), apparently without overt toxicity. However, M2 elicits severe, amantadine-reversible cytotoxicity when expressed in cells cultivated in weakly acidic media such as insect cells (Schroeder et al. 1994a) and *S. cerevisiae* (Kurtz et al. 1995). Membrane rafts exist in both these systems (Puertollano et al. 1997; Rietveld et al. 1999; Bagnat et al. 2000). Cleverley et al. (1997) reported that when M2 was expressed in insect cells cholesterol-depleted through several passages, a treatment which disintegrates rafts, its amantadine-suppressible cytotoxic effect was abolished, suggesting a role for cholesterol in M2 function.

Here we investigate the cholesterol association of the M2 protein isolated from influenza virus-infected cells and insect cells. We have previously shown that M2 protein hyperexpressed in insect cells exhibited the normal host-cell modifications, phosphorylation and palmitoylation, and supported amantadine- and rimantadine-sensitive proton translocation when reconstituted into proteoliposomes (Schroeder et al. 1994a; Lin et al. 1997; Lin and Schroeder 2001). M2 expressed in *E. coli* was included as a cholesterol-free control. We find that cholesterol associates with the M2 protein but is nonessential for its proton-channel activity, cytotoxicity and inhibition by rimantadine. A cholesterol-binding motif is located in the post-transmembrane region of the M2 endodomain. We propose that M2 has dual affinity to raft and non-raft membranes, which

directs it to the raft periphery and may underlie its role in virus assembly and budding.

Materials and methods

Viruses and cell culture

Influenza A/Germany/27 (H7N7, Weybridge) was propagated in embryonated hens' eggs; primary chick embryo cells were grown in minimal essential medium with fetal calf serum (FCS; Biochrom). CFM2 is a recombinant baculovirus with the Weybridge M2 gene cloned under the polyhedron promoter (Schroeder et al. 1994a); *Trichoplusia ni* Hi 5-hyperexpressing insect cells were originally purchased from JRH Biosciences.

M2 isolation from influenza virus-infected cells labeled with tritiated cholesterol

Chick cells (3×10^7) were plated in the presence of FCS and labeled overnight with 150–250 μCi 1,2,6,7-^{3}H(*N*)-cholesterol (NEN). The labeling medium was removed, the monolayers washed twice with minimal essential medium and infected at a multiplicity of infection of 5–10 plaque-forming units per cell. At 7 h post-infection, monolayers were washed twice with PBS and extracted 30 min on ice with 9 ml extraction buffer (ExB; 50 mM Tris-HCl, 150 mM NaCl, 1% NP40, 1 mM EDTA and a protease inhibitor cocktail; Schroeder et al. 1994a). The extract was cleared 15 min in an Eppendorf centrifuge at full speed at 4 °C and applied to a column of anti-M2 ectodomain IgG coupled to UltraLink (Pierce). The column was washed with 20 vol ExB, followed by 10 vol ExB-OG (the same buffer with 40 mM 1-octyl-β-D-glucopyranoside) until the disappearance of tritium counts. The wash was continued with 20 mM morpholinopropanesulfonic acid, 40 mM OG, pH 5.5, until the disappearance of tritium counts. Elution was with 10 vol glycine-HCl, 40 mM OG, pH 2.8, and fractions were immediately neutralized with 1/10 vol 1 M Tris-HCl, pH 8.0, 40 mM OG. The pooled eluates were concentrated through Centricon 30 and Microcon 30 devices (Millipore). M2 content was determined by comparative dot blotting using an M2 standard purified from insect cells. The cholesterol concentration of the chick-cell extract was determined enzymatically with the Amplex Red assay (Molecular Probes). The cholesterol content of M2 preparations was calculated from the ^{3}H counts recovered in the cholesterol spot after thin-layer chromatography of the neutral lipid extract (see below).

Expression and purification of influenza M2 protein from insect cells

M2 was expressed from *T. ni* cells infected with the recombinant baculovirus CFM2 and purified from the cleared detergent extract of the total cell membranes (following removal of peripheral membrane proteins by a 1 M KCl wash) by immunoaffinity FPLC as described (Schroeder et al. 1994a; Lin and Schroeder 2001). The total membranes were extracted with 1% TX-100 in Hepes-buffered saline (HBS; 150 mM NaCl, 10 mM Hepes, pH 7.8) and the extract applied to an Ultralink column (Pierce) coupled to rabbit IgG specific to the M2-ectodomain. Washes with 6 vol 1 and 2% TX-100, 1 M NaCl in HBS preceded detergent exchange with 6 vol HBS, 40 mM OG, 1 M NaCl. In some cases this was followed by an extended wash with HBS, 40 mM OG. M2 was eluted at pH 2.8 with 15 vol 100 mM glycine-HCl buffer and 40 mM OG. The eluate fractions were immediately neutralized with Tris, pooled and concentrated.

Cloning, expression and purification of his$_6$-tagged M2 protein from *E. coli*

A PCR fragment containing the Weybridge M2 sequence (aa 2–97) was extended by PCR to introduce an *N*-terminal sequence MAH$_6$GSIEGR and cloned between the *Nco*I and the *Eco*RI site of pTRC99A (Pharmacia) in *E. coli* SCS110 (Stratagene). M2-expressing clones were selected for rimantadine-dependent growth by parallel plating on LB agar with IPTG (0.050–1 mM) with and without rimantadine (25 μM). Sequence-confirmed clone Nx8′ was used for the production of his-tagged M2 in the presence of rimantadine, following IPTG (250 μM) induction. M2 purification from *E. coli* is based on the purification scheme of HIV Vpu (Ewart et al. 1996). Osmotically sensitized *E. coli* cells ("ghosts"), prepared according to Varadhachary and Maloney (1990), were extracted on ice for 1 h with 1% taurodeoxycholate (TDC) in 20 mM sodium phosphate buffer, 250 mM NaCl, pH 7.3, 10 mM 2-mercaptoethanol, 1 mM EDTA, 20% glycerol. Next, 1 mM $MgCl_2$, 200 μg/ml DNAse and 20 μg/ml RNAse were added and the extract cleared at 50,000 rpm at 4 °C in the TST60.4 rotor, concentrated fivefold through Centrifree (Millipore) and cleared again for 30 min at 4 °C at full speed in the Eppendorf centrifuge. The concentrate was made 10 mM in imidazole and applied to 200 μl Ni-NTA magnetic beads (Qiagen) per gram of cells. The beads were washed three times with 2 ml buffer (supplemented with 1% TDC, 1% glycerol, 20 mM imidazol), followed by three washes with 0.4 ml 250 mM imidazole in 100 mM sodium citrate, 330 mM Na_2HPO_4, pH 6.0, 250 mM NaCl, 1% glycerol, 1 mM EDTA and 10 mM 2-mercaptoethanol. TDC was exchanged for OG by washing with 3×0.2 ml 40 mM OG in the same buffer (without glycerol), followed by elution with 200 μl of 1.25 M imidazole and immediate rebuffering into KPSOG (12 mM potassium phosphate buffer, 50 mM K_2SO_4, pH 7.4, 40 mM OG) in Microcon 30 concentrators (Millipore). M2 concentration was determined by dot blotting compared to an M2 standard. A

protease-inhibitor cocktail (Schroeder et al. 1994a) was present throughout, except during elution of M2.

Binding to cholesteryl hemisucccinate agarose

Cholesteryl hemisuccinate (CHS) was immobilized on diaminodipropylamine agarose (Pierce) with 1-ethyl-3-(3-dimethylaminopropyl)carbodiimide in 75% dioxane, based on the method of Wichman (1979) and the instructions of the supplier. At the same time, diaminodipropylamine agarose was reacted without CHS to serve as a control for nonspecific binding. The gels were washed extensively with 75% dioxane, 1 M NaCl and HBS, 40 mM OG, with and without 1 M NaCl. Next, 0.3 µg M2 were incubated in 1.5 ml low-retention polystyrene tubes (Axygen) with 10 µl gel in 100 µl 10 mM Hepes, pH 7.8, containing 1.15 M NaCl, 40 mM OG, 1 mM dithiothreitol (DTT) and 0.02% NaN_3 in a thermomixer (Eppendorf) at 1,000 rpm for 2 h at 4 °C. The gels were recovered by filtration through Ultrafree centrifugal filters (0.22 µm; Millipore), transferred into fresh low-retention tubes containing 1 ml incubation buffer (4 °C), washed three times for 5 min at a thermomomixer setting of 1,400 rpm and finally extracted with double-strength Laemmli buffer (2% SDS, 40 mM DTT) for 5 min at 96 °C.

Filipin staining of protein-bound cholesterol

Purified M2 protein was subjected to native gel electrophoresis at 70 mA through 1% agarose gels (HGT(P), Biozym, Germany) in sodium barbital buffer (Sigma) at pH 8.3 on ice. Gels were fixed at room temperature in 7.5% trichloroacetic acid, washed three times with PBS and stained overnight with 4 mg filipin (filipin complex, F9765, Sigma) in 50 ml PBS, as described by Smejkal and Hoff (1994). Gels were inspected on a UV transilluminator and images recorded with a video system (Südlabor, Germany). The filipin-stained gel was subsequently stained with colloidal Coomassie (GELCODE Blue Stain Reagent; Pierce) and evaluated by densitometry with the program PCBAS 2.09 (Raytest, Germany) using the profiles routine on a manually adjusted background line. Calculations are based on the free cholesterol content of the HDL/LDL standard (1.46 nmol/µl). Images were processed with Adobe Photoshop 4.0.

Membrane reconstitution of M2

For proton translocation assays, 60 µg *T. ni* M2 or 90 µg *E. coli* M2 protein was reconstituted with 1 mg lipids. The complex lipid mixture (Wharton et al. 1986) consisted of phosphatidylcholine (Sigma P9513), sphingomyelin (S7004), phosphatidylethanolamine (P8704), phosphatidylserine (P6641), phosphatidylinositol (P0639), gangliosides (G9886) and cholesterol (C8667) (molar ratio 10:3:3:1:0.5:0.32:14); the cholesterol-free lipid mixture (DMPC/PS) consisted of 0.85 mg L-α-dimyristoylphosphatidylcholine (DMPC; P6392) and 0.15 mg phosphatidylserine (Dencher et al. 1986). Both lipid mixtures contained 0.2 mol% valinomycin, a potassium ionophore. Liposomes were formed by sequential dialysis against KPS as described (Schroeder et al. 1994a). The pH-probe pyranine (2.2 mM) was introduced with the first two dialysis buffers.

For studying model DRM, 50 µg M2 protein was reconstituted with 2 mg of the complex lipid mixture and dialyzed overnight against 5 l KPS. The liposomes were extracted with 1 ml 1% TX-100 in KPS for 1 h at 4 °C and centrifuged for 1.5 h at 36,000 rpm in the TST60.4 rotor in a Beckman L7 ultracentrifuge. The pellet was resuspended in KPS, made 50% in sucrose, overlayed with 30% and 5% sucrose in KPS and centrifuged overnight at 45,000 rpm in the TST60.4 rotor. Fractions were dot blotted for M2 and evaluated by densitometry.

M2 proton-channel assay

Proton translocation was assayed as described in Lin and Schroeder (2001). Briefly, buffers and liposomes were equilibrated at 18 °C. Reactions were started by introducing liposomes made up in KPS into NaPS, pH 7.4 (12 mM sodium phosphate buffer, 50 mM Na_2SO_4) with or without rimantadine. Proton translocation was driven by the K^+ diffusion potential (Schroeder et al. 1994a). Readings of pyranine fluorescence at 510 nm excited at dual wavelengths, 410 and 460 nm, were taken with an SLM AB2 fluorimeter (Aminco-Bowman) at 1 s intervals. The internal pH is proportional to the emission ratio (Dencher et al. 1986).

Lipid extraction and thin-layer chromatography

The lipids from 50 µl concentrated eluates from immunoaffinity chromatography of ^{3}H-cholesterol-labeled M2 were extracted according to Bligh and Dyer (1959). The concentrated methanol-chloroform extract was applied to a silica gel G thin-layer sheet (Merck). Standards of cholesterol, oxidized sterols and cholesterol esters were run in parallel in 80% heptane, 20% ether, 1% formic acid. The dried TLC sheet was developed with primulin. Spots visualized under a UV lamp were cut out, placed in a scintillation cuvette and moistened with heptane before adding 5 ml scintillation cocktail.

Results

Influenza M2 protein associates with cholesterol

M2 protein was isolated from three distinct systems, virus-infected primary host cells, a high-expression

baculovirus-insect cell system, and bacteria. M2 was purified by immunoaffinity chromatography, utilizing IgG raised against an *N*-terminal peptide, or in the case of bacterially expressed M2, Ni-NTA chromatography. Primary chick embryo cells were pre-labeled with ^{3}H-cholesterol and infected with influenza virus. Before elution of IgG-bound M2 at pH 2.8 an additional wash at pH 5.5 was introduced to dissociate any M1 complexes (Ruigrok et al. 2000). Tritium counts in each column wash and during detergent exchange from TX-100 to 1-octyl-β-D-glucopyranoside (OG) were monitored and each step continued until the tritium counts declined to background level. The pH 2.8 eluate contained 2,540 dpm and roughly 60 ng M2, estimated by comparative dot blotting. A methanol-chloroform extract of this fraction containing the neutral lipids (1,830 dpm) was analyzed by thin-layer chromatography along with standards of cholesterol, oxidized cholesterols and cholesterol ester (Table 1). Sixty-nine percent of the label was recovered from the cholesterol spot, while 12% remained at the origin with certain oxidized sterols. For comparison, the analysis was also performed on the pH 5.5 wash, which contained somewhat less cholesterol but significantly more oxidized cholesterols. It is likely that this material was associated with the M1 protein (cp. Ruigrok et al. 2000), but the pH 5.5 wash also contained some M2 (data not shown). The cholesterol content of virally expressed M2 was estimated on the basis of the cholesterol content of the labeled cells and the specific activity of the label to be about 0.9 molecules per M2 monomer (Table 2).

Baculovirus-expressed influenza M2 protein from insect (*T. ni*) cells was purified by immunoaffinity FPLC to near homogeneity (Lin and Schroeder 2001) and its cholesterol content was analyzed by sequential staining with filipin and Coomassie blue (Smejkal and Hoff 1994). Filipin is a fluorescent macrolide that binds stoichiometrically to sterols with a 3β-OH group (Schroeder et al. 1972). M2-protein preparations were subjected to native electrophoresis on 1% agarose gels on ice. Among several native gel systems tested, this was the only one in which M2 migrated as a single band (Lin and Schroeder 2001), making it suitable for lipid staining and allowing the high protein load required for visualizing protein-associated cholesterol (Fig. 1a). Based on the free-cholesterol content of high- and low-density lipoprotein (HDL/LDL) concentration standards (Fig. 1, lanes 7, 8), these M2 protein preparations were estimated to contain 0.5 cholesterol molecules per monomer (Table 2). *E. coli*-expressed M2 was included in the

Table 1 Thin-layer chromatography of a neutral lipid extract of M2 isolated from ^{3}H-cholesterol-labeled virus-infected cells. Neutral lipid extracts of concentrated affinity-purified M2 (pH 2.8 eluate) and of the pH 5.5 wash of the material bound to the affinity column were mixed with standards and analyzed by thin layer chromatography. Lanes were subdivided into zones (mm) corresponding to the standards and intervening area, and were scraped off and assayed by scintillation counting

Zone	(mm)	Molecular species	pH 2.8 eluate (M2)		pH 5.5 wash	
			(dpm)	(%)	(dpm)	(%)
1	0 ± 3.8	Oxidized sterols[a]	169	12.3	785	40.0
2	3.8–16.1		65	4.7	104	5.3
3	16.1–25.2	Cholesterol	956	69.3	871	44.4
4	25.2–29.2		23	1.7	38	1.9
5	29.2–37.8	3-Keto-4-cholestene-3-one	35	2.5	22	1.1
6	37.8–47.3		12.5	0.9	46	2.3
7	47.3–57.3		36	2.6	24	1.2
8	57.3–69.8	3-Keto-5α-cholestane-3-one	9	0.7	14	0.7
9	69.8–95.3		13	0.9	20	1.0
10	95.3–122.8		10	0.7	19	1.0
11	122.8–147.8		12.5	0.9	10	0.5
12	147.8–163.8	Cholesterol ester	38	2.8	10	0.5

[a]7β-Hydroxycholesterol, 20 α-hydroxycholesterol, 25-hydroxycholesterol

Table 2 Cholesterol content of M2 preparations

Assay	Cell system	M2 expression (virus/plasmid)	M2 (pmol tetramer)	Cholesterol (pmol)	Cholesterol/M2 monomer
^{3}H-cholesterol incorporation	CEC	Influenza virus	1.3	4.6	0.9[a]
Filipin staining	*T.ni* Hi5	Baculovirus[b] I	244	519	0.53[c]
		II	193	426	0.55[c]
	E.coli	p *TRC99A* Nx8′	101	28	0.07[c]

[a]Data from a representative labeling experiment (cf. Table 1)
[b]*I* and *II* are independent preparations of insect cell-expressed M2
[c]Estimate based on densitometry of Coomassie and filipin staining of M2 bands in agarose gels (Fig. 1)

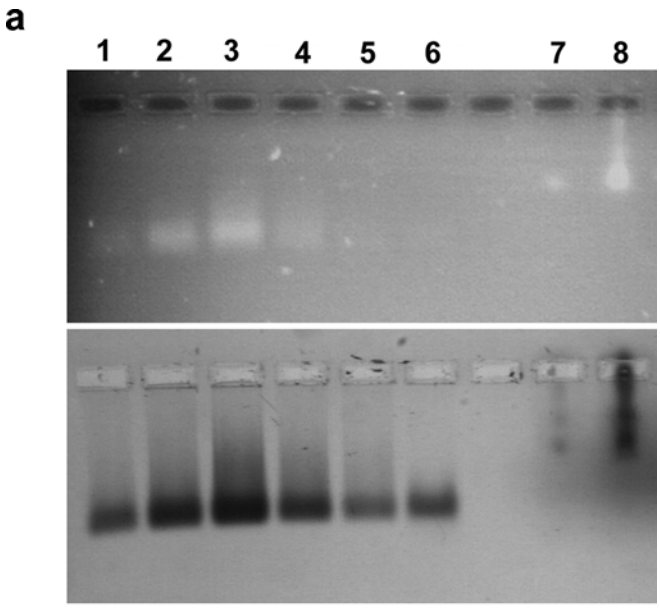

Fig. 1a, b Filipin staining of influenza M2 protein-bound cholesterol. **a** M2 preparations run on agarose gel stained with filipin (*top*), followed by Coomassie staining (*bottom*). *Lane 1* M2 (preparation II) 4 µg, *2* M2 (II) 8.8 µg, *3* M2 (preparation I) 11 µg, *4* M2 (I) 5.6 µg, *5* M2 (I) 2.8 µg, *6 E. coli* M2 5.7 µg, *7* LDL/HDL cholesterol standard 0.07 µl and *8* 0.25 µl. **b** Comparative densitometry of filipin and Coomassie staining. *r.d.* Relative density. Data points used for estimation of M2 cholesterol content (Table 2) are labeled. *Regression lines* were fitted using Excel

analysis as a background control (lane 6). Details on bacterial M2 expression are given below.

The cholesterol affinity of the M2 protein was further investigated by binding to cholesteryl hemisuccinate (CHS) agarose. Using this method, Vincent et al. (2002) demonstrated cholesterol binding of the pre-TM sequence of soluble HIV gp41 fragments. By prolonging the detergent exchange from TX-100 to OG of insect cell-expressed M2 (bound to the immunoaffinity-FPLC column) by washing with 15 column vol OG buffer in the absence or presence of NaCl, the cholesterol content

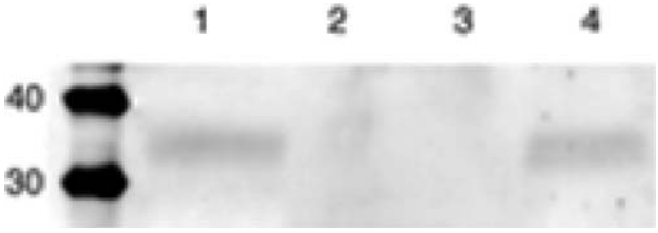

Fig. 2 Capture of the M2 protein on solid phase-bound cholesterol. M2 was bound to cholesterylhemisuccinate (CHS) agarose or control agarose for 2 h at 4 °C and washed extensively. The gels were extracted with SDS sample buffer. Molecular weight markers 30 and 40 kDa. *Lane 1* M2 control (dimer), *2* empty, *3* control agarose, *4* CHS agarose

could be lowered to about 0.1 molecules per M2 tetramer (data not shown). Insect-cell M2 with low cholesterol content was incubated for 2 h at 4 °C with CHS and control agarose, and binding was analyzed by PAGE and Western blotting (Fig. 2). M2 protein was recovered from CHS agarose but not from control agarose, suggesting specific binding of M2 to the cholesteryl group. Due to harsh binding and washing conditions there was extensive denaturation (data not shown) which prevented a quantitative evaluation of binding. Thus the procedure, which was developed for soluble proteins (Vincent et al. 2002), requires optimization for membrane proteins.

M2 expression in a cholesterol-free system induces rimantadine-suppressible cytotoxicity

M2 has been previously expressed in *E. coli* and shown to be cytotoxic (Guinea and Carrasco 1994), without the relationship of toxicity to ion-channel activity having been stringently established with an M2-specific ion-channel blocker. We cloned M2 under the non-leaky IPTG-inducible *trc* promoter of p *Trc*99A in *E. coli* SCS110 and plated transformed cells in the presence of rimantadine (25 µM). Colonies were subsequently analyzed by plating in parallel with and without rimantadine. All clones selected by their total inability to plate in the absence of rimantadine were found to express the M2 protein. Clearly, the M2 ion channel was cytotoxic in *E. coli*, an intrinsically cholesterol-free system.

In this construct, the *N*-terminal methionine is followed by a hexahistidine tag and a factor-X cleavage site (MH_6GSIEGR), preceding serine 2 as the first authentic M2 amino acid. *E. coli*-expressed M2 was extracted from bacterial ghosts with 1% taurodeoxycholate as described in Materials and methods. M2 was purified to near homogeneity, and taurodeoxycholate was exchanged for 40 mM OG by Ni-NTA chromatography. Since the factor-Xa cleavage product proved unstable, *E. coli* M2 preparations retaining the *N*-terminal extension were studied. Figure 3 shows a comparative Western blot of bacterially expressed and insect cell-expressed M2. Both form partially SDS- and DTT-refractive dimers and

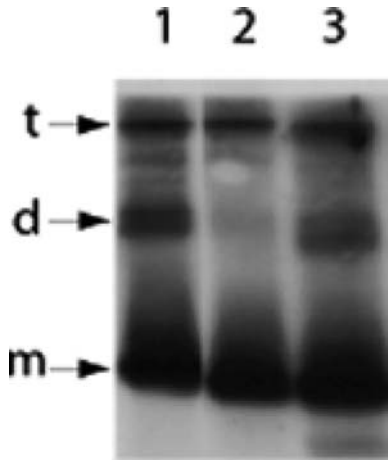

Fig. 3 Electrophoretic mobility of *E. coli*-expressed M2 protein. M2 protein isolated from insect cells (*lane 2*) and from *E. coli* (*lanes 1* and *3*) was analyzed by SDS polyacrylamide gel electrophoresis and Western blot. *Lane 3 E. coli* M2 cleaved by factor Xa. The blot was developed with an antibody directed to a C-terminal peptide of M2. *m* Monomer, *d* dimer, *t* tetramer

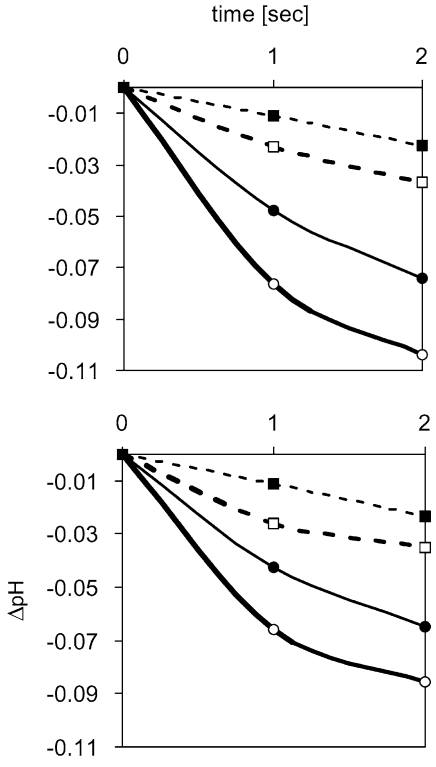

Fig. 4 Proton translocation activity of M2 protein expressed in *Trichoplusia ni* and *E. coli*. Proteins were reconstituted into cholesterol-free (DMPC/PS) (*above*) or cholesterol-rich raft proteoliposomes (*below*). Reactions were initiated by introducing proteoliposomes into incubation buffer with or without 1 μM rimantadine and recorded by dual wavelength fluorimetry of the incorporated pH indicator pyranine. Internal pH was calculated from emission ratios. ΔpH Internal pH minus internal pH at $t = 0$. *Open squares* represent *E. coli* M2, *closed squares E.coli* M2 plus 1 μM rimantadine, *open circles* represent insect-cell M2, *closed circles* insect-cell M2 plus 1 μM rimantadine. Plotted data are the average of three to five recordings

tetramers, also following factor-Xa cleavage, dimers being more prominent in *E. coli* than in insect-cell M2. Tetramers are the minimal structural unit of M2 ion-channel activity (Sakaguchi et al. 1997). Like M2 from insect cells, *E. coli* M2 forms a single band on native agarose gels (Fig. 1a). Judged by Coomassie staining of SDS-polyacrylamide gels, *E. coli*-expressed M2 was more than 95% pure (data not shown). The causes of its impaired stability and activity are not yet understood, e.g. the composition of the *E. coli* membrane, the detergent taurodeoxycholate or the free SH group on cysteine 50 (palmitoylated in eukaryotic cells).

M2 inserts into membranes and translocates protons in the absence of cholesterol

A possible cholesterol requirement for the M2 ion-channel activity was previously addressed by comparing cholesterol-containing ("raft") and cholesterol-free (DMPC/PS) liposomes, reconstituted with 500 or 100 molecules of insect cell-expressed M2. Nearly identical proton translocation activities emerged, 7.7 vs. 7.3 protons per second per M2 tetramer at neutral pH, and 25.7 vs. 17.2 (18 °C, difference not significant) at the weakly acidic pH 5.7 which activates the channel (Lin and Schroeder 2001). Conditions in these experiments were not absolutely cholesterol-free, since the reconstituted M2 protein purified from insect cells contained about 0.5 mol cholesterol per mol M2 monomer (cf. Table 2). We therefore attempted functional reconstitution of cholesterol-free M2 purified from *E. coli*.

The activity of N-terminally tagged M2 prepared from *E. coli* and M2 purified from insect cells was compared. Both displayed rimantadine-sensitive proton translocation in cholesterol-free as well as in cholesterol-containing liposomes (Fig. 4). While the specific activity of purified *E. coli* M2 was at least five times lower than that of *T. ni* M2, cholesterol was not essential for membrane incorporation, ion-channel function or the rimantadine sensitivity of the protein. The seemingly lower activity of M2 in cholesterol-containing liposomes is a consequence of their larger volume, compared to the cholesterol-free liposomes (Lin and Schroeder 2001).

Detergent resistance of membrane-reconstituted M2 protein

Membrane–raft association is operationally defined as resistance to extraction with 1% Triton X-100 (TX-100) or CHAPS at 4 °C (Fiedler et al. 1993). Artificial membranes serve as experimental models of lateral phase separation (Ahmed et al. 1997) and the TX-100 insolubility of membrane microdomains and their associated proteins (Schroeder et al. 1994b, 1998; Brown and London 1998). We studied the partition of insect cell- and *E. coli*-expressed M2 into synthetic raft membranes.

The complex lipid mixture was the same as used in the functional reconstitution of M2 (see above). The proportion of cholesterol (44 mol%) and sphingomyelin (9.4 mol%), similar to MDCK PM (Hansson et al. 1986) and influenza-virus membranes (Zhang et al. 2000b), is compatible with the formation of detergent-insoluble microdomains (Sankaram and Thompson 1990; Schroeder et al. 1994b). Reconstituted M2 proteoliposomes were extracted with 1% TX-100 at 4 °C and pelleted, the pellets re-homogenized and subjected to sucrose gradient flotation. While only 5–8% of the liposomal M2 protein became TX-100-insoluble, this material partitioned nearly quantitatively into the detergent-resistant membranes floating in the upper half of the gradient (Fig. 5). There was no significant difference in the behavior of *T. ni*- and *E. coli*-expressed M2, except that the latter was more prone to precipitation.

Discussion

Cholesterol is not essential for the ion-channel function and cytotoxicity of M2 tetramers

M2 from virus-infected chick cells as well as from an insect-cell expression system purified with bound cholesterol. The detergent OG efficiently solubilizes integral raft proteins refractive to TX-100 at 4 °C (Hooper and Turner 1988; Brown and Rose 1992; Avalos et al. 1997) in particular influenza hemagglutinin (Kurzchalia et al. 1992), and released influenza M1 and NP (Zhang and Lamb 1996; Avalos et al. 1997) from the cytoskeleton. The M2-cholesterol complex survived washes of the FPLC column with 2% TX-100 and with OG in the presence of 1 M NaCl but gradually dissociated by extended washing with OG. Thus, cholesterol appears to bind M2 noncovalently.

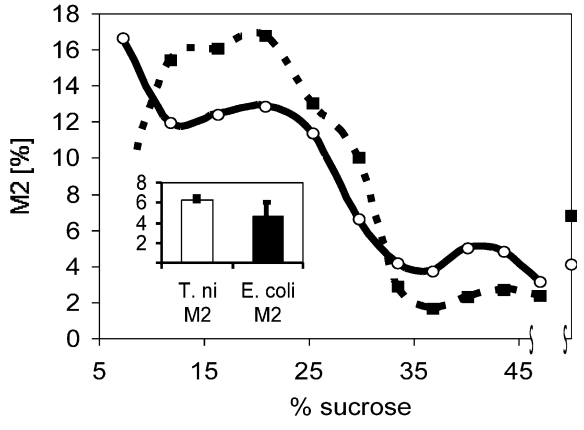

Fig. 5 Flotation analysis of M2 incorporated into detergent-resistant membrane. Evaluation by dot blotting and densitometry (averages from two experiments). M2 protein preparations were reconstituted into raft liposomes, extracted with 1% TX-100 at 4 °C and pelleted by ultracentrifugation. *Inset* Percent of M2 in TX-100-insoluble pellets. Resuspended pellets were run on sucrose gradients. *Main panel* Sucrose gradient fractions. *Squares* represent *E. coli* M2, *circles* insect-cell (*T. ni*) M2. *Points on far right* M2 precipitated through sucrose gradient

In previous functional studies of reconstituted M2, a low level of protein-associated cholesterol was inadvertently introduced into initially cholesterol-free lipid vesicles. To probe the significance of this, M2 was expressed in a sterol-free system (*E. coli*), isolated, and reconstituted into model membranes in the presence or absence of cholesterol. There are, as far as we know, no published ion-channel recordings of *E. coli*-expressed M2. Cholesterol proved nonessential for tetramerization of *E. coli* M2, for its membrane reconstitution, ion-channel activity and inhibition by rimantadine.

In *E. coli* the M2 protein elicited specific, rimantadine-suppressible cytotoxicity, indicating that it was functional and that cholesterol was dispensable for its ion-channel activity and cytotoxicity in vivo. This also extends to the M2 modifications absent in *E. coli*, phosphorylation and palmitoylation, agreeing with previous observations (Holsinger et al. 1995) on their nonessential nature for M2 ion-channel activity in *Xenopus* oocytes. Hennessy et al. (1993) found that M2 expressed in *E. coli* was disposed in the cytoplasmic membrane with its ectodomain in the low-pH periplasm. This is the orientation, N-terminal to C-terminal with respect to the pH gradient, in which M2 translocates protons. The likely cause of M2 toxicity to *E. coli* is therefore the dissipation of the proton electrochemical gradient.

Heterologous cell systems in which the expression of wild-type M2 is overtly toxic have in common a pH gradient at the cytoplasmic membrane. In *S. cerevisiae* where M2 is also toxic, it is the proton electrochemical gradient as well (Kurtz et al. 1995), while in insect cells cultivation at pH 6 imposes a pH gradient at the plasma membrane. M2 is more active at pH < 7 (Pinto et al. 1992; Chizhmakov et al. 1996) and correspondingly more cytotoxic. An M2 mutant with relaxed ion selectivity (Wang et al. 1995) was also far more cytotoxic to vertebrate cells (Smith et al. 2002), apparently by dissipating not only pH but also other ion gradients.

Cleverley et al. (1997) found that cholesterol depletion reduced the toxicity of M2 to *Sf9* insect cells; they inferred a role for cholesterol in M2 ion-channel activity which our data does not support. A recent study showing that the tetramerization of an M2 TM fragment is optimal in bilayers of Golgi thickness (C16-C18 phospholipids) and compromised in bilayers composed of short phospholipids may resolve the contradiction. Inclusion of cholesterol into the latter enhanced membrane thickness and tetramerization (Cristian et al. 2003). Insect-cell (grown at 27 °C) membranes are generally composed of shorter phospholipids than membranes of cells grown at 37 °C (Rietveld et al. 1999), and both *Sf9* (Gimpl et al. 1995) and *T. ni* grown in the presence of cholesterol (Marheineke et al. 1998) have a cholesterol-to-phospholipid ratio seven-times lower than mammalian cells. Thus, cholesterol depletion, which significantly altered *Sf9* Golgi morphology (Cleverley

et al. 1997), may have impaired M2 tetramerization, the precondition of channel activity (Sakaguchi et al. 1997). However, cholesterol seems not to be required for Golgi function and targeting in *Aedes albopictus* cells (Rolls et al. 1997). The lower stability of *E. coli* M2 and its higher dimer content (compare Fig. 3) may be similarly related to suboptimal tetramerization conditions in *E. coli*.

Membrane-binding properties and lipid-binding motifs of the post-TM sequence of M2

Similar to HIVgp41 pre-TM (Suárez et al. 2000), the M2 post-TM sequence has a high interfacial hydrophobicity extending ten residues beyond the transmembrane domain (Fig. 6a), recently confirmed by NMR of M2 proteoliposomes (Tian et al. 2003). Apart from the transmembrane domain, which has been shown not to bind cholesterol (Cristian et al. 2003), the post-TM sequence is the only other hydrophobic area of the M2 protein, making it a potential cholesterol-binding site. M2 was captured by solid phase-bound cholesterol (cf. Fig. 2). Vincent et al. (2002) used CHS agarose to delimit the cholesterol-binding region of HIV gp41, in which LWYIK corresponds to the cholesterol recognition/interaction amino acid consensus (CRAC), L/V-$X_{(1–5)}$-Y-$X_{(1–5)}$-R/K, of the peripheral-type benzodiazepine receptor (Li and Papadopoulos 1998; Li et al. 2001).

M2 exhibits CRAC motifs immediately downstream of the transmembrane domain located at the cytoplasmic face of the PM or the virus interior (Fig. 6b). In HIV gp41 the motif is located immediately adjacent but upstream of the TM domain, facing the extracellular space and the HIV exterior (Vincent et al. 2002). The first CRAC motif present in most sequenced M2 proteins encompasses the palmitoylation site (C50). In a majority of human influenza strains there is only one motif and in the strain A/Udorn the consensus is violated (Fig. 6b), but the impact of such variations on cholesterol binding remains to be investigated.

The HIV gp41 pre-TM peptide encompassing the CRAC motif is required for the fusion of HIV with host cells (Muñoz-Barroso et al. 1999; Salzwedel et al. 1999); it associates with raft domains and forms pores in a cholesterol- and sphingomyelin-dependent manner (Sáez-Cirión et al. 2002). Analogously, the M2 post-TM region may be involved in cholesterol binding and membrane restructuring during virus morphogenesis.

Fig. 6a, b M2 protein hydrophobic sequence elements. **a** Hydrophobicity and interfacial hydrophobicity plots. Hydrophobicity (*grey*) was calculated according to Kyte and Doolittle (1982), interfacial hydrophobicity (*black*) according to White and Whimley (1999) for a window of 11 amino acids centered on the indicated residue. **b** Sequence motifs in the transmembrane (TM) and post-TM region. M2 subsequences of representative human (*Sing 1/57*; A/Singapore 1/57 H2N2, accession number CAA30893 and *Udorn 307/72*; A/Udorn 307/72 H3N2, accession number P03490) and an avian influenza virus strain (*Weybridge*; influenza A/Germany/27 H7N7 Weybridge, accession number L37797) are shown. Residues conserved in all accessible sequences are in *bold* print, those more than 90% conserved are *underlined*. The discernable motifs are indicated *above*, key amino acids of the CRAC motifs with *grey shading*. Within the M2 sequences, CRAC motifs are enhanced by *grey shading*. *Palm* palmitoylation site, *YRxL/F* internalization motif (see text)

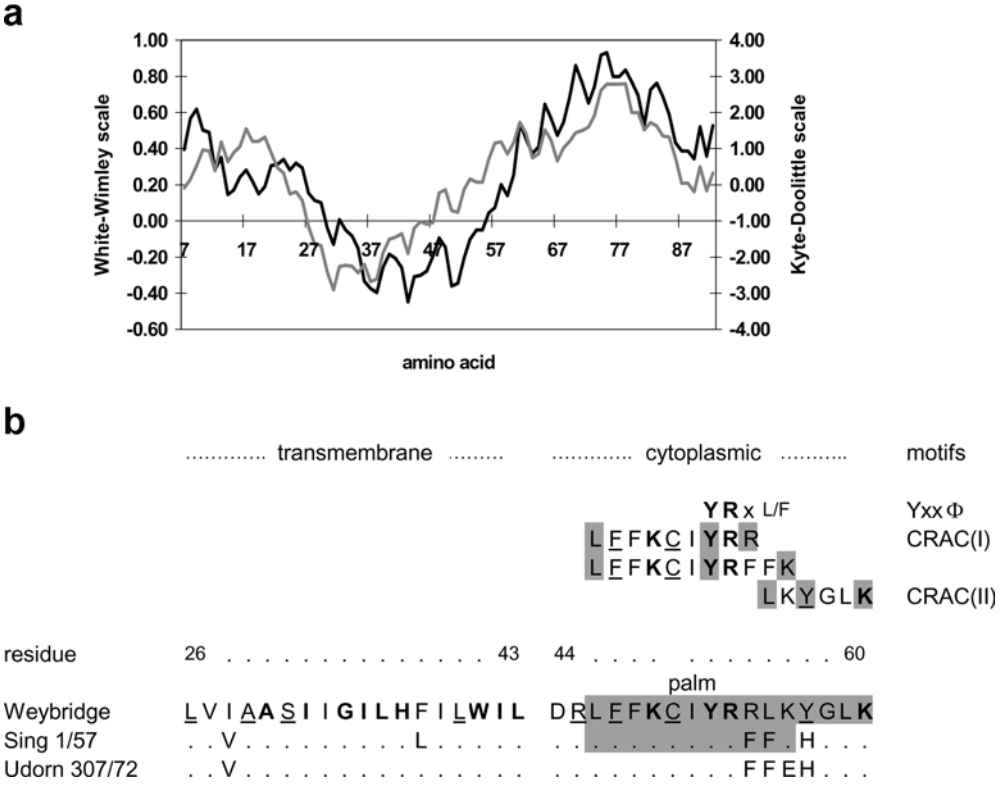

Furthermore, the post-TM sequence of M2 Weybridge (Fig. 6b) is remarkably homologous to the XIP region of Na/Ca exchangers: **DR**rl**L***F<u>Y</u><u>K</u>Y*-<u>V</u>***Y***K****R***Y<u>R</u>**AG** (accession number AAD26362). Bold print represents identical residues, underscoring represents functionally related residues. CRAC motif residues are followed by an asterisk. Apart from two amino acids (minor case), the two align perfectly with respect to the preceding TM segments and endocytic internalization motifs (represented by italics; Collawn et al. 1990). The basic amino acids of the M2 post-TM sequence have been predicted to interact with acidic phospholipid headgroups at the membrane–water interface (Kochendoerfer et al. 1999; Saldanha et al. 2002). This is corroborated by the specific affinity of the XIP region for phosphatidylinositol 4,5-bisphosphate (He at al. 2000). Of note, the cytoplasmic leaflet of raft membranes is enriched for phosphatidylinositol 4,5-bisphosphate (Liu et al. 1998). Therefore, the M2 post-TM sequence bears overlapping motifs implicated in determining affinity to raft lipids.

Whereas HA and NA are integral raft proteins (Skibbens et al. 1989; Kurzchalia et al. 1992; Kundu et al. 1996; Scheiffele et al. 1997; Harder et al. 1998), it is argued that M2, consistent with its low concentration in detergent-resistant membranes, exhibits dual targeting to non-raft and raft domains. Membrane rafts accumulate cholesterol, growing thicker as they progress towards the PM (Coxey et al. 1993; Ren et al. 1997). Proteins residing in or recycling to the Golgi generally have shorter TM regions than those targeted to the PM (Munro 1995; Webb et al. 1998), e.g. the 26- to 29-amino acid TM segments of HA and NA. Combining a short TM segment like the 19-amino acid M2 TM helix (Lamb et al. 1985) rooted in non-raft membrane with an interfacially hydrophobic post-TM helix carrying a palmitate moiety extended into rafts may fix M2 at the raft–non-raft interface (Fig. 7a). The geometry of M2 α-helices in this figure is roughly based on NMR spectroscopy of pure M2 protein (Tian et al. 2003). Similarly, it has been proposed that human acetylcholine esterase is targeted to the raft edge due to the presence of a saturated and a polyunsaturated lipid modification (Schroeder et al. 1998).

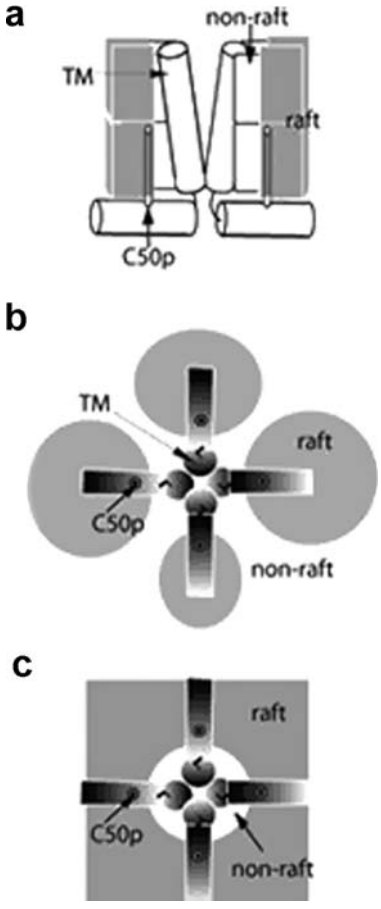

Fig. 7a–c Membrane association of the M2 tetramer. **a** A slice through the M2 protein shows two of the four TM segments embedded in non-raft membrane. The tilt of the TM and post-TM α-helices is according to M2 NMR data (Tian et al. 2003). The palmitate modification of C50 (*C50p*) is shown inserting into raft membrane. **b** View of the M2 tetramer from the endodomain. The post-TM regions bridge separate membrane rafts. **c** Following merger of the rafts, the tetramer is trapped in a small patch of non-raft membrane within a larger raft domain

A model of the role of M2 in virus assembly and budding

Cholesterol affinity of M2 may determine the co-localization with HA and NA observed throughout apical transport (Sugrue et al. 1990b; Ciampor et al. 1992a, 1992b; Grambas et al. 1992; Ohuchi et al. 1994; Takeuchi and Lamb 1994) ultimately leading to its low-level incorporation into budding virus as construed in the following model. The model is developed from four lines of investigation: (1) the role of M2 in determining the shape of virus particles, (2) the role of rafts in influenza-envelope protein traffic and budding, (3) our findings on M2 cholesterol-binding and (4) lipid-binding properties and the flexibility of the M2 post-TM sequence as predicted by NMR and molecular modeling. The core tenet is dual membrane domain targeting of M2, by its TM segment to non-raft and by post-TM determinants to rafts, defining a peripheral raft protein.

Zhang et al. (2000b) pointed out that the under-representation of M2 in the virion reflects its exclusion from rafts. The firm association of M2 with the matrix (Bron et al. 1993), the essential function of M2 in virus uncoating demonstrated by amantadine sensitivity (Kato and Eggers 1969; Takeda et al. 2002), and its role in virus morphogenesis argue for a mechanism specifically incorporating M2 molecules in the virion.

Obvious steric constraints prohibit all four palmitate chains on an M2 tetramer from engaging with the same raft, but they might bridge separate rafts and promote raft merger (Fig. 7). The extent of peripheral lipid insertion should increase with decreasing domain edge

curvature and be maximal when curvature is reversed as non-raft membrane is completely surrounded by raft membrane (Fig. 7c). Thus, dual membrane domain affinity may enable M2 to promote coalescence of membrane microdomains into larger arrays and to stabilize patches of non-raft membrane within rafts.

Efficient budding of fully infectious influenza virus involves interactions of the three envelope proteins and the matrix (M1) protein (Latham and Galarza 2001) and their raft association (Scheiffele et al. 1999; Zhang et al. 2000a, 2000b). M1 is the major driving force of morphogenesis, in that it is necessary (Lohmeyer et al. 1979) and sufficient (Gomez-Puertas et al. 2000) for the budding of virus-like particles. In contrast, budding and raft association are compromised but not completely prevented by deleting cytoplasmic sequences of HA and NA (Jin et al. 1997; Zhang et al. 2000b). HA palmitoylation improves raft targeting (Melkonian et al. 1999) and virus budding (Jin et al. 1996), but the significance of M2 palmitoylation for virus budding is unknown. Rafts originate as small dynamic structures, which grow and are fortified by lateral cross-linking (cf. review Harder 2001). M2 may provide a focus of attachment of M1/RNP which will in turn cluster microdomains bearing envelope proteins (cf. review Nayak and Barman 2002) entrapping some M2 molecules in raft membrane (Fig. 7c).

Lamb et al. (1985) predicted that M2 is likely to play a role in organizing the assembly of the virion. There is mutational evidence (Zebedee and Lamb 1988, 1989; Roberts et al. 1998) of physical interaction between the M1 and M2 proteins during virus budding: antibodies to the M2 *ecto*domain (Zebedee and Lamb 1988) but not Fab domains (Hughey et al. 1995) inhibit the release of progeny viruses and shift the balance in favor of spherical particles, suggesting the importance of cross-linking adjacent M2 molecules. Mutants and strains resistant to these antibodies exhibit substitutions in either M1 or M2 (Zebedee and Lamb 1989) and a preponderance of the spherical or the filamentous morphology (Roberts et al. 1998). Antibodies cross-linking M2 *ecto*domains appear to influence interactions on the other side of the membrane between the M2 endodomain and M1.

As the virus bud is extruded, M2 protein will be driven from the shrinking raft (envelope) periphery into surrounding non-raft membrane causing an increase in local M2 concentration. Finally, nascent virus particles are connected to the PM by a membranous tube (for a review see Garoff et al. 1998), short in the case of influenza virus (compare electron micrographs in Hughey et al. 1995; Lamb and Krug 1996). The pre-fission budding pore is shown schematically in Fig. 8a. The M2 post-TM sequence is modeled as an α-helical extension of the TM domain making a tight 90° turn at Asp44-Arg45 and binding to the inner leaflet (Kochendoerfer et al. 1999; Saldanha et al. 2002; Tian et al. 2003). M2 molecules at the edge of the envelope may engage in a three-point interaction with M1, with raft and non-raft membrane. M2 tethered within the matrix should be pulled into a membrane-normal orientation and dynamic transitions of M2-membrane interactions via alternative lipid-binding modes of the post-TM and TM domain may trigger membrane restructuring and fission (Fig. 8a). Turns in the M2 post-TM sequence at the YxxΦ motif (Collawn et al. 1990) or a loop following Gly58 (Saldanha et al. 2002) would provide the necessary flexibility. Membrane fission and rearrangement of M2 clusters at the narrowing lipid domain boundary may seal and segregate viral and cell membranes and deposit a few M2 molecules at the vestigial "navel" of the viral envelope within a narrow zone of non-raft membrane (Figs. 7c, 8b).

The fact that antibodies to the M2 ectodomain promote the formation of spherical particles (Hughey et al. 1995; Roberts et al. 1998) may be rationalized by their

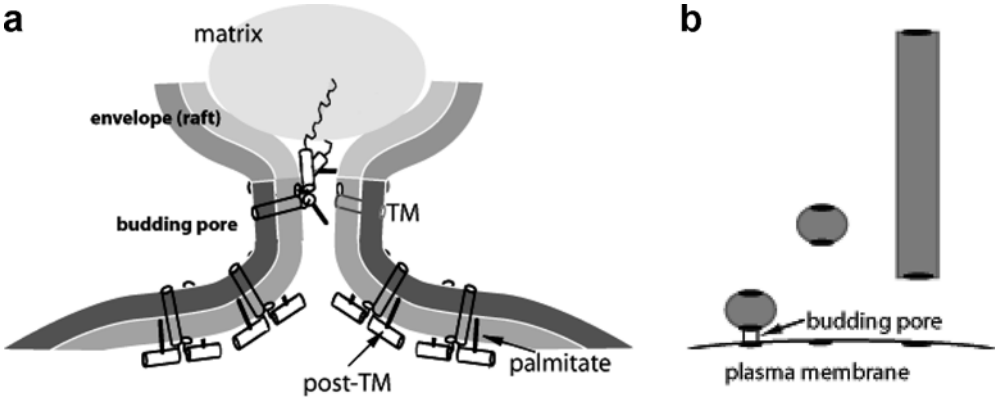

Fig. 8a, b Model of M2 function during fission at the budding pore. **a** The *budding pore* at the initiation of fission. M2 molecules have been driven out of the nascent envelope into adjacent non-raft membrane. M2 *TM* and *post-TM* regions and *palmitate* groups are indicated. The locations of α-helices and turns are based on molecular modeling (Kochendorfer et al. 1999; Saldanha et al. 2002). An M2 tetramer at the edge of the budding *envelope* is depicted in the process of structural rearrangement. Its endodomains are tethered in the matrix. One palmitate moiety is shown inserted into the inner leaflet of the envelope, one is about to insert across the pore lumen and another has disengaged from non-raft membrane. **b** Rearrangements of M2 molecules may promote pinching-off and sealing of the segregating viral and plasma membrane where M2 clusters (*black*) are left behind. Spherical and filamentous particles are not drawn to scale

gathering the M2 tetramers into a ring constricting the budding pore and accelerating fission, similar to dynamin and other proteins forming rings around membranous tubes (for a review see Huttner and Zimmerberg 2001). The drawing (Fig. 8b) depicts spherical and filamentous buds just before fission. M2 is shown at one or both ends of the bud, the latter version assuming that the long M2 endodomain formed the initial focus associating with the matrix. The proposed budding mechanism, in agreement with published EM images of immunogold-labeled M2 clustered at the neck of virus buds (Hughey et al. 1995; Lamb and Krug 1996), may produce virions with distinct pole(s) of M2 clusters.

Acknowledgements C.S. expresses her gratitude to Prof. Nikolaus Müller-Lantzsch and Prof. Friedrich Graesser at the Department of Virology of the University of the Saarland in Homburg. The authors are grateful for advice from and critical discussion with Drs. Barry Ely and Stephen A. Wharton, and thank Alan J. Hay (National Institute for Medical Research, London, U.K.) for the gift of antisera. We are indebted to Drs. Bernd Rüstow (Surfactant Laboratory of the Charité) for his support of lipid analysis and Brigitte Brux (Protein Analytics Laboratory of the Charité) for advice on cholesterol assays and native gels. Prof. Andreas Herrmann generously granted access to fluorimeters at the Institute of Biophysics, Humboldt University. Nadine Hardel helped with the cloning and Kathlen Schröder is thanked for reliable technical assistance. This work was supported by the Deutsche Forschungsgemeinschaft (grant No. Schr 554/2) and the Charité Berlin (project No. 98-273).

References

Ahmed SN, Brown DA, London E (1997) On the origin of sphingolipid/cholesterol-rich detergent-insoluble cell membranes: physiological concentrations of cholesterol and sphingolipid induce formation of a detergent-insoluble, liquid-ordered lipid phase in model membranes. Biochemistry 36:10944–10953

Armstrong RT, Kushnir AS, White JM (2000) The transmembrane domain of influenza hemagglutinin exhibits a stringent length requirement to support the hemifusion to fusion transition. J Cell Biol 151:425–37

Asano K, Asano A (1988) Binding of cholesterol and inhibitory peptide derivatives with the fusogenic hydrophobic sequence of F-glycoprotein of HVJ (Sendai virus): possible implication in the fusion reaction. Biochemistry 27:1321–1329

Avalos RT, You Z, Nayak DP (1997) Association of influenza virus NP and M1 proteins with cellular cytoskeletal elements in influenza virus-infected cells. J Virol 71:2947–2958

Bagnat M, Keränen S, Shevchenko A, Shevchenko A, Simons K (2000) Lipid rafts function in biosynthetic delivery of proteins to the cell surface in yeast. Proc Natl Acad Sci USA 97:3254–3259

Barman S, Ali A, Hui EK, Adhikary L, Nayak DP (2001) Transport of viral proteins to the apical membranes and interaction of matrix protein with glycoproteins in the assembly of influenza viruses. Virus Res 77:61–69

Bligh ED, Dyer WJ(1959) A rapid method of total lipid extraction and purification. Can J Biochem Physiol 37:911–917

Briggs JAG, Wilk T, Fuller SD (2003) Do lipid rafts mediate virus assembly and pseudotyping? J Gen Virol 84:757–768

Bron R, Kendal AP, Klenk HD, Wilschut J (1993) Role of the M2 protein in influenza virus membrane fusion: effects of amantadine and monensin on fusion kinetics. Virology 195:808–811

Brown DA, London E (1998) Functions of lipid rafts in biological membranes. Annu Rev Cell Dev Biol 14:111–136

Brown DA, Rose JK (1992) Sorting of GPI-anchored proteins to glycolipid-enriched membrane subdomains during transport to the apical cell surface. Cell 68:533–544

Chizhmakov IV, Geraghty FM, Ogden DC, Hayhurst A, Antoniou M, Hay AJ (1996) Selective proton permeability and pH regulation of the influenza virus M2 channel expressed in mouse erythroleukemia cells. J Physiol 494:329–336

Ciampor F, Bayley PM, Nermut MV, Hirst EMA, Sugrue RJ, Hay AJ (1992a) Evidence that the amantadine-induced, M2-mediated conversion of influenza A virus haemagglutinin to the low pH conformation occurs in an acidic trans Golgi compartment. Virology 188:14–24

Ciampor F, Thompson CA, Hay AJ (1992b) Regulation of pH by the M2 protein of influenza A viruses. Virus Res 22:247–258

Cleverley DZ, Geller HM, Lenard J (1997) Characterization of cholesterol-free insect cells infectible by baculoviruses: effects of cholesterol on VSV fusion and infectivity and on cytotoxicity induced by influenza M2 protein. Exp Cell Res 233:288–296

Collawn JF, Stangel M, Kuhn LA, Esekogwu V, Jing S, Trowbridge IS, Tainer JA (1990) Transferrin receptor internalization sequence YXRF implicates a tight turn as the structural recognition motif for endocytosis. Cell 63:1061–1072

Coxey RA, Pentchev PG, Campbell G, Blanchette-Mackie EJ (1993) Differential accumulation of cholesterol in Golgi compartments of normal and Niemann-Pick type C fibroblasts incubated with LDL: a cytochemical freeze-fracture study. J Lipid Res 34:1165–1176

Cristian L, Lear JD, DeGrado WF (2003) Use of thiol-disulfide equilibria to measure the energetics of assembly of transmembrane helices in phospholipid bilayers. Proc Natl Acad Sci USA 100:14772–14777

Dencher NA, Burghaus PA, Grzesiek S (1986) Determination of the net proton-hydroxide ion permeability across vesicular lipid bilayers and membrane proteins by optical probes. Methods Enzymol 127:746–760

Ewart GD, Sutherland T, Gage PW, Cox GB (1996) The Vpu protein of human immunodeficiency virus type 1 forms cation-selective ion channels. J Virol 70:7108–7115

Fiedler K, Kobayashi T, Kurzchalia TV, Simons K (1993) Glycosphingolipid-enriched, detergent-insoluble complexes in protein sorting in epithelial cells. Biochemistry 32:6365–6373

Fischer WB, Sansom MSP (2002) Viral ion channels: structure and function. Biochim Biophys Acta 1561:27–45

Garoff H, Hewson R, Opstelten DE (1998) Virus maturation by budding. Microbiol Mol Biol Rev 62:1171–1190

Gimpl G, Klein U, Reiländer H, Fahrenholz F (1995) Expression of oxytocin receptor in baculovirus-infected insect cells: high affinity binding is induced by a cholesterol-cyclodextrin complex. Biochemistry 34:13794–13801

Gómez-Puertas P, Albo C, Pérez-Pastrana E, Vivo A, Portela A (2000) Influenza virus matrix protein is the major driving force in virus budding. J Virol 74:11538–11547

Grambas S, Hay AJ (1992) Maturation of influenza A virus haemagglutinin—estimates of the pH encountered during transport and its regulation by the M2 protein. Virology 190:11–18

Guinea R, Carrasco L (1994) Influenza virus M2 protein modifies membrane permeability in *E. coli* cells. FEBS Lett 343:242–246

Hansson GC, Simons K, van Meer G (1986) Two strains of the Madin-Darby canine kidney (MDCK) cell line have distinct glycosphingolipid compositions. EMBO J 5:483–489

Harder T (2001) Raft membrane domains and immunoreceptor functions. Adv Immunol 77:45–92

Harder T, Scheiffele P, Verkade P, Simons K (1998) Lipid domain structure of the plasma membrane revealed by patching of membrane components. J Cell Biol 141:929–942

Hay AJ (1992) The action of adamantanamines against influenza A viruses: inhibition of the M2 ion channel protein. Semin Virol 3:21–30

He Z, Feng S, Tong Q, Hilgemann DW, Philipson KD (2000) Interaction of PIP(2) with the XIP region of the cardiac Na/Ca exchanger. Am J Physiol Cell Physiol 278:C661-C666

Henkel JR, Weisz OA (1998) Influenza M2 protein slows traffic along the secretory pathway; pH perturbation of acidified compartments affects early Golgi transport steps. J Biol Chem 273:6518–6524

Henkel JR, Gibson GA, Poland PA, Ellis MA, Hughey RP, Weisz OA (2000) Influenza M2 proton channel activity inhibits *trans*-Golgi network release of apical membrane and secreted proteins in polarized Madin-Darby canine kidney cells. J Cell Biol 148:495–504

Hennessey ES, Hashemzadeh-Bonehi L, Hunt LA, Broome-Smith JK (1993) Assembly of eukaryotic class III (N-out, C-in) membrane proteins into the *Escherichia coli* cytoplasmic membrane. FEBS Lett 331:159–161

Holsinger LJ, Lamb RA (1991) Influenza virus M2 integral membrane protein is a homotetramer stabilized by formation of disulphide bonds. Virology 183:32–43

Holsinger LJ, Shaughnessy MA, Micko A, Pinto LH, Lamb RA (1995) Analysis of posttranslational modifications of the influenza virus M2 protein. J Virol 69:1219–1225

Hooper NG, Turner AJ (1988) Ectoenzymes of the kidney microvillar membrane. Biochem J 250:865–869

Hughey PG, Compans RW, Zebedee SL, Lamb RA (1992) Expression of the influenza A virus M2 protein is restricted to apical surfaces of polarized epithelial cells. J Virol 66:5542–5552

Hughey PG, Roberts PC, Holsinger LJ, Zebedee SL, Lamb RA, Compans RW (1995) Effects of antibody to the influenza A virus M2 protein on M2 surface expression and virus assembly. Virology 212:411–421

Huttner WB, Zimmerberg J (2001) Implications of lipid microdomains for membrane curvature, budding and fission. Curr Opin Cell Biol 13:478–484

Ingham PW (2000) Hedgehog signaling: how cholesterol modulates the signal. Curr Biol 10:R180-R183

Jin H, Subbarao K, Bagal S, Leser GP, Murphy BR, Lamb RA (1996) Palmitylation of the influenza virus hemagglutinin (H3) is not essential for virus assembly or infectivity. J Virol 70:1406–1414

Jin H, Leser GP, Zhang J, Lamb RA (1997) Influenza hemagglutinin and neuraminidase cytoplasmic tails control particle shape. EMBO J 16:1236–1247

Kato N, Eggers HJ (1969) Inhibition of uncoating of fowl plague virus by 1-adamantanamine hydrochloride. Virology 37:632–641

Keller P, Simons K (1998) Cholesterol is required for surface transport of influenza virus hemagglutinin. J Cell Biol 140:1357–1367

Kochendoerfer GG, Salom D, Lear JD, Wilk-Orescen R, Kent SBH, DeGrado WF (1999) Total synthesis of the integral membrane protein influenza A virus M2: role of its C-terminal domain in tetramer assembly. Biochemistry 38:11905–11913

Kundu A, Avalos RT, Sanderson CM, Nayak DP (1996) Transmembrane domain of influenza virus neuraminidase, a type II protein, possesses an apical sorting signal in polarized MDCK cells. J Virol 70:6508–6515

Kurtz S, Luo G, Hahnenberger KM, Brooks C, Gecha O, Ingalls K, Numata K, Krystal M (1995) Growth impairment resulting from expression of influenza virus M2 protein in *Saccharomyces cerevisiae*: identification of a novel inhibitor of influenza virus. Antimicrob Agents Chemother 39:2204–2209

Kurzchalia TV, Dupree P, Parton RG, Kellner R, Virta H, Lehnert M, Simons K (1992) VIP21 a 21–kD membrane protein is an integral component of *trans*-Golgi-network-derived transport vesicles. J Cell Biol 118:1003–1014

Kyte J, Doolittle RF (1982) A simple method for displaying the hydropathic character of a protein. J Mol Biol 157:105–132

Lamb RA, Krug RM (1996) Orthomyxoviridae: the viruses and their replication. In: Fields BN, Knipe DM, Howley PM, Chanock RM, Melnick JL, Monath TP, Roizman B, Straus SE (eds) Fields virology, 3rd edn. Lippincott-Raven, Philadelphia, pp 1353–1395

Lamb RA, Zebedee SL, Richardson CD (1985) Influenza virus M2 protein is an integral membrane protein expressed on the infected cell surface. Cell 40:627–633

Lamb RA, Holsinger LJ, Pinto LH (1994) The influenza A virus M2 ion channel protein and its role in the influenza virus life cycle. In: Wimmer E (ed) Cellular receptors of animal viruses. Cold Spring Harbor Laboratory, Cold Spring Harbor, pp 303–321

Latham T, Galarza JM (2001) Formation of wild-type and chimeric influenza virus-like particles following simultaneous expression of only four structural proteins. J Virol 75:6154–6165

Li H, Papadopoulos V (1998) Peripheral-type benzodiazepine receptor function in cholesterol transport. Identification of a putative cholesterol recognition/interaction amino acid sequence and consensus pattern. Endocrinology 139:4991–4997

Li H, Yao Z, Degenhardt B, Teper G, Papadopoulos V (2001) Cholesterol binding at the cholesterol recognition/interaction amino acid consensus (CRAC) of the peripheral-type benyodiazepine receptor and inhibition of steroidogenesis by an HIV TAT-CRAC peptide. Proc Natl Acad Sci USA 98:1267–1272

Lin T, Schroeder C (2001) Definitive assignment of proton selectivity and attoampere unitary current to the M2 ion channel protein of influenza A virus. J Virol 75:3647–3656

Lin S, Naim HY, Rodriguez AC, Roth MG (1998) Mutations in the middle of the transmembrane domain reverse the polarity of transport of the influenza virus hemagglutinin in MDCK epithelial cells. J Cell Biol 142:51–57

Lin T, Heider H, Schroeder C (1997) Different modes of inhibition by adamantane amine derivatives and natural polyamines of the functionally reconstituted influenza virus M2 proton channel protein. J Gen Virol 78:767–774

Liu Y, Casey L, Pike LJ (1998) Compartmentalization of phosphatidylinositol 4,5-bisphosphate in low-density membrane domains in the absence of caveolin. Biochem Biophys Res Commun 245:684–690

Lohmeyer J, Talens LT, Klenk HD (1979) Biosynthesis of influenza virus envelope in abortive infection. J Gen Virol 42:73–88

Manié SN, Debreyne S, Vincent S, Gerlier D (2000) Measles virus structural components are enriched into lipid raft microdomains: a potential cellular location for virus assembly. J Virol 74:305–311

Marheineke K, Grünewald S, Christie W, Reiländer H (1998) Lipid composition of *Spodoptera frugiperda* (Sf9) and *Trichoplusia ni* (T.n) insect cells used for baculovirus infection. FEBS Lett 441:49–52

Melkonian KA, Ostermeyer AG, Chen JZ, Roth MG, Brown DA (1999) Role of lipid modifications in targeting proteins to detergent-resistant membrane rafts. J Biol Chem 274:3910–3917

Monier S, Dietzen DJ, Hastings WR, Lublin DM, Kurzchalia TV (1996) Oligomerization of VIP21-caveolin in vitro is stabilized by long chain fatty acylation or cholesterol. FEBS Lett 388:143–149

Mould JA, Drury JE, Frings SM, Kaupp UB, Pekosz E, Lamb RA, Pinto LH (2000) Permeation and activation of the M2 ion channel of influenza A virus. J Biol Chem 275:31038–31050

Muñoz-Barroso I, Salzwedel K, Hunter E, Blumenthal R (1999) Role of the membrane-proximal domain in the initial stages of human immunodeficiency virus type I envelope glycoprotein-mediated membrane fusion. J Virol 73:6089–6092

Munro S (1995) An investigation of the role of transmembrane domains in Golgi protein retention. EMBO J 14:4695–4704

Murata M, Peränen J, Schreiner R, Wieland F, Kurzchalia TV, Simons K (1995) VIP21/caveolin is a cholesterol-binding protein. Proc Natl Acad Sci USA 92:10339–10343

Nayak DP, Barman S (2002) Role of lipid rafts in virus assembly and budding. Adv Virus Res 58:1-28

Ohuchi M, Cramer A, Vey M, Ohuchi R, Garten M, Klenk HD (1994) Rescue of vector-expressed fowl plague virus hemagglutinin in biologically active form by acidotropic agents and coexpressed M2 protein. J Virol 68:920–926

Parks GD, Lamb RA (1991) Topology of eukaryotic type II membrane proteins: importance of *N*-terminal positively charged residues flanking the hydrophobic domain. Cell 64:777–787

Pepinsky RB, Zheng C, Wen D, Rayhorn P, Baker DP, Williams KP, Bixler SA, Ambrose CM, Garber EA, Miatkowski K, Taylor FR, Wang EA, Galdes A (1998) Identification of a palmitic acid-modified form of human sonic hedgehog. J Biol Chem 273:14037–14045

Pickl WF, Pimentel-Muiños FX, Seed B (2001) Lipid rafts and pseudotyping. J Virol 75:7175–7183

Pinto LH, Holsinger LJ, Lamb RA (1992) Influenza virus M2 protein has ion channel activity. Cell 69:517–528

Porter JA, Young KE, Beachy PA (1996) Cholesterol modification of hedgehog signaling domains in animal development. Science 274:255–259

Puertollano R, Li S, Lisanti MP, Alonso MA (1997) Recombinant expression of the MAL proteolipid, a component of glycolipid-enriched membrane microdomains, induces the formation of vesicular structures in insect cells. J Biol Chem 272:18311–18317

Ren J, Lew S, Wang Z, London E (1997) Transmembrane orientation of hydrophobic alpha-helices is regulated both by the relationship of helix length to bilayer thickness and by cholesterol concentration. Biochemistry 36:10213–10220

Rietveld A, Neutz S, Simons K, Eaton S (1999) Association of sterol- and glycosylphosphatidylinositol-linked proteins with Drosophila raft lipid microdomains. J Biol Chem 274:12049–12054

Roberts PC, Compans RW (1998) Host cell dependence of viral morphology. Proc Natl Acad Sci USA 95:5746–51

Roberts PC, Lamb RA, Compans RW (1998) The M1 and M2 proteins of influenza virus are important determinants in filamentous particle formation. Virology 240:127–137

Rolls MM, Marquardt MT, Kielian M, Machamer CE (1997) Cholesterol-independent targeting of Golgi membrane proteins in insect cells. Mol Biol Cell 8:2111–2118

Ruigrok RWH, Barge A, Durrer P, Brunner J, Ma K, Whittaker GR (2000) Membrane interaction of influenza virus M1 protein. Virology 267:289–298

Sáez-Cirión A, Nir S, Lorizate M, Agirre A, Cruz A, Pérez-Gil J, Nieva JL (2002) Sphingomyelin and cholesterol promote HIV gp41 pretransmembrane sequence surface aggregation and membrane restructuring. J Biol Chem 277:21776–21785

Sakaguchi T, Leser GP, Lamb RA (1996) The ion channel activity of the influenza virus M2 protein affects transport through the Golgi apparatus. J Cell Biol 133:733–747

Sakaguchi T, Tu Q, Pinto LH, Lamb RA (1997) The active oligomeric state of the minimalistic influenza virus M2 ion channel is a tetramer. Proc Natl Acad Sci USA 94:5000–5005

Saldanha JW, Czabotar PE, Hay AJ, Taylor WR (2002) A model for the cytoplasmic domain of the influenza A virus M2 channel by analogy to the HIV-1 vpu protein. Protein Pept Lett 9:495–502

Salzwedel K, West JT, Hunter E (1999) A conserved tryptophan-rich motif in the membrane-proximal region of the human immunodeficiency virus type 1 gp41 ectodomain is important for Env-mediated fusion and virus infectivity. J Virol 73:2469–2480

Sanderson CM, Avalos R, Kundu A, Nayak DP (1995) Interaction of Sendai viral F, HN and M proteins with host cytoskeletal and lipid components in Sendai virus-infected BHK cells. Virology 209:701–707

Sankaram MB, Thompson TE (1990) Modulation of phospholipid acyl chain order by cholesterol. A solid-state 2H nuclear magnetic resonance study. Biochemistry 29:10676–10684

Scheiffele P, Roth MG, Simons K (1997) Interaction of influenza virus haemagglutinin with sphingolipid-cholesterol membrane domains via its transmembrane domain. EMBO J 16:5501–5508

Scheiffele P, Rietveld A, Wilk T, Simons K (1999) Influenza viruses select ordered lipid domains during budding from the plasma membrane. J Biol Chem 274:2038–2044

Schmidt MFG (1982) Acylation of viral spike glycoproteins: a feature of enveloped RNA viruses. Virology 116:327–338

Schroeder F, Holland JF, Bieber LL (1972) Fluorometric investigations of the interaction of polyene antibiotics with sterols. Biochemistry 11:3105–3111

Schroeder C, Ford CF, Wharton SA, Hay AJ (1994a) Functional reconstitutition in lipid vesicles of influenza virus M2 protein expressed by baculovirus: evidence for proton transfer activity. J Gen Virol 75:3477–3484

Schroeder R, London E, Brown D (1994b) Interactions between saturated acyl chains confer detergent resistance on lipids and glycosylphosphatidylinositol (GPI)-anchored proteins: GPI-anchored proteins in liposomes and cells show similar behaviour. Proc Natl Acad Sci USA 91:12130–12134

Schroeder RJ, Ahmed SN, Zhu Y, London E, Brown DA (1998) Cholesterol and sphingolipid enhance the Triton X-100 insolubility of glycosylphosphatidylinositol-anchored proteins by promoting the formation of detergent-insoluble ordered membrane domains. J Biol Chem 273:1150–1157

Simons K, Ikonen E (1997) Functional rafts in cell membranes. Nature 387:569–572

Skibbens JE, Roth MG, Matlin KS (1989) Differential extractability of influenza virus hemagglutinin during intracellular transport in polarized epithelial cells and nonpolar fibroblasts. J Cell Biol 108:821–832

Smejkal GB, Hoff HF (1994) Filipin staining of lipoproteins in polyacrylamide gels: sensitivity and photobleaching of the fluorophore and its use in a double staining method. Electrophoresis 15:922–925

Smith CA, Graham CM, Mathers K, Skinner A, Hay AJ, Schroeder C, Thomas DB (2002) Conditional ablation of T-cell development by a novel viral ion channel transgene. Immunology 105:306–313

Suárez T, Gallaher WR, Agirre A, Goñi FM, Nieva JL (2000) Membrane interface-interacting sequences within the ectodomain of the human immunodeficiency virus type 1 envelope glycoprotein: putative role during viral fusion. J Virol 74:8038–8047

Sugrue RJ, Hay AJ (1991) Structural characteristics of the M2 protein of influenza A viruses: evidence that it forms a tetrameric channel. Virology 180:617–624

Sugrue RJ, Belshe RB, Hay AJ (1990a) Palmitoylation of the influenza A virus M2 protein. Virology 179:51–56

Sugrue RJ, Bahadur G, Zambon MC, Hall-Smith M, Douglas AR, Hay AJ (1990b) Specific structural alteration of the influenza haemagglutinin by amantadine. EMBO J 9:3469–3476

Takeda M, Pekosz A, Shuck K, Pinto LH, Lamb RA (2002) Influenza A virus M2 ion channel activity is essential for efficient replication in tissue culture. J Virol 76:1391–1399

Takeuchi K, Lamb RA (1994) Influenza virus M2 protein ion channel activity stabilizes the native form of fowl plague virus hemagglutinin during intracellular transport. J Virol 68:911–919

Thiele C, Hannah MJ, Fahrenholz F, Huttner W (2000) Cholesterol binds to synaptophysin and is required for biogenesis of synaptic vesicles. Nature Cell Biol 2:42–49

Tian D, Gao PF, Pinto LH, Lamb RA, Cross TA (2003) Initial structure and dynamic characterization of the M2 protein transmembrane and amphipathic helices in lipid bilayers. Protein Sci 12:2597–2605

Varadhachary A, Maloney PC (1990) A rapid method for reconstitution of bacterial membrane proteins. Mol Microbiol 4:1407–1411

Veit M, Klenk HD, Rott R, Kendal A (1991) The M2 protein of influenza A virus is acylated. J Gen Virol 72:1461–1465

Vincent N, Genin C, Malvoisin E (2002) Identification of a conserved domain of the HIV-1 transmembrane protein gp41 which interacts with cholesteryl groups. Biochim Biophys Acta 1567:157–164

Wang C, Lamb RA, Pinto LH (1995) Activation of the M2 ion channel of influenza virus, a role for the transmembrane domain histidine residue. Biophys J 69:1363–1371

Webb RJ, East JM, Sharma RP, Lee AG (1998) Hydrophobic mismatch and the incorporation of peptides into lipid bilayers: a possible mechanism for retention in the Golgi. Biochemistry 37:673–679

Wharton SA, Skehel JJ, Wiley DC (1986) Studies of influenza haemagglutinin-mediated membrane fusion. Virology 149:27–35

White SH, Wimley WC (1999) Membrane protein folding and stability: physical principles. Annu Rev Biophys Biomol Struct 28:319–365

Whittacker GR, Helenius A (1998) Nuclear import and export of viruses and virus genomes. Virology 246:1-23

Whittacker GR, Bui M, Helenius A (1996) The role of nuclear import and export in influenza virus infection. Trends Cell Biol 6:67–71

Wichman A (1979) Affinity chromatography of human plasma low- and high-density lipoproteins. Elution by selective cleavage of a bond in the spacer. Biochem J 181:691–698

Zebedee SL, Lamb RA (1988) Influenza A virus M2 protein: monoclonal antibody restriction of virus growth and detection of M2 in virions. J Virol 62:2762–2772

Zebedee SL, Lamb RA (1989) Growth restriction of influenza A virus by M2 protein antibody is genetically linked to the M1 protein. Proc Natl Acad Sci USA 86:1061–1065

Zebedee SL, Richardson CD, Lamb RA (1985) Characterization of the influenza virus M2 integral membrane protein and expression at the infected-cell surface from cloned cDNA. J Virol 56:502–511

Zhang J, Lamb RA (1996) Characterization of the membrane association of the influenza virus matrix protein in living cells. Virology 225:255–266

Zhang J, Leser GP, Pekosz A, Lamb RA (2000a) The cytoplasmic tails of the influenza virus spike glycoproteins are required for normal genome packaging. Virology 269:325–334

Zhang J, Pekosz A, Lamb RA (2000b) Influenza virus assembly and lipid raft microdomains: a role for the cytoplasmic tails of the spike glycoproteins. J Virol 74:4634–4644